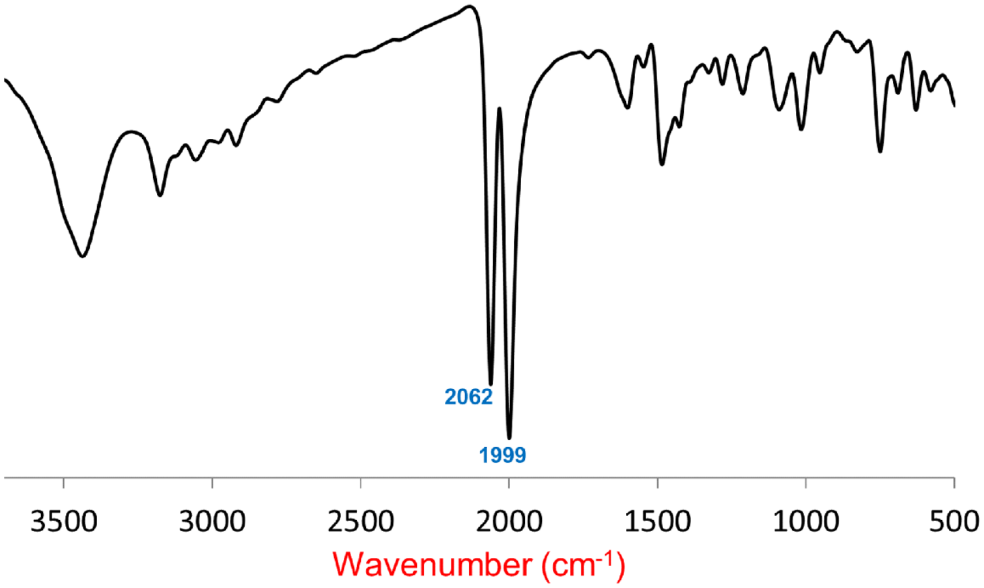
2062
1999
3500
3000
2500
2000
1500
1000
500
Wavenumber (cm$^{-1}$)

a)

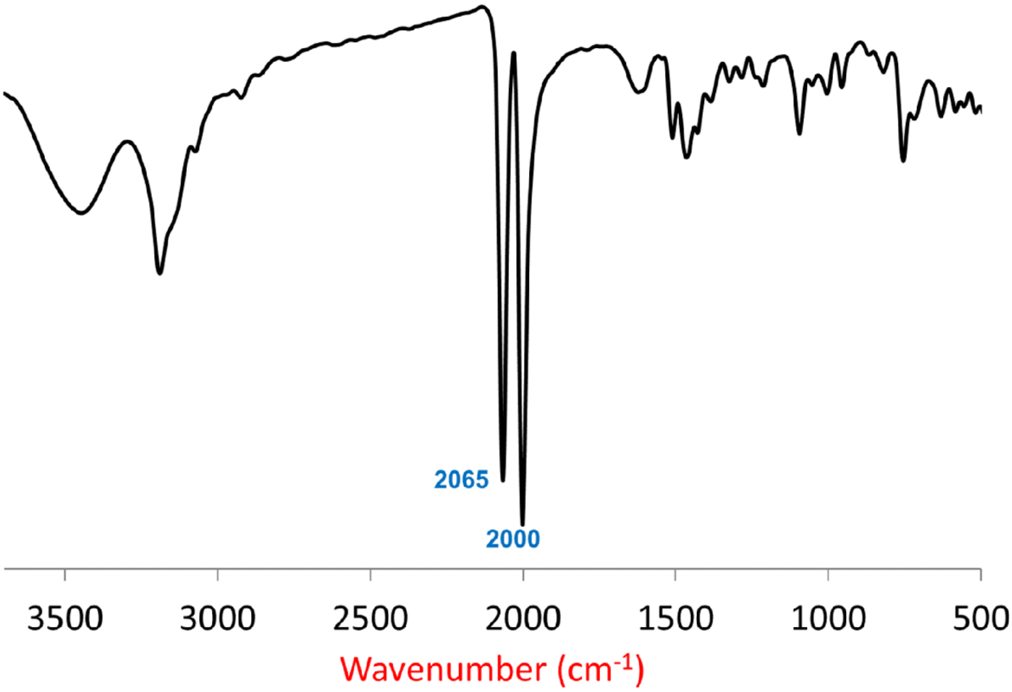
2065
2000
3500
3000
2500
2000
1500
1000
500
Wavenumber (cm$^{-1}$)

b)

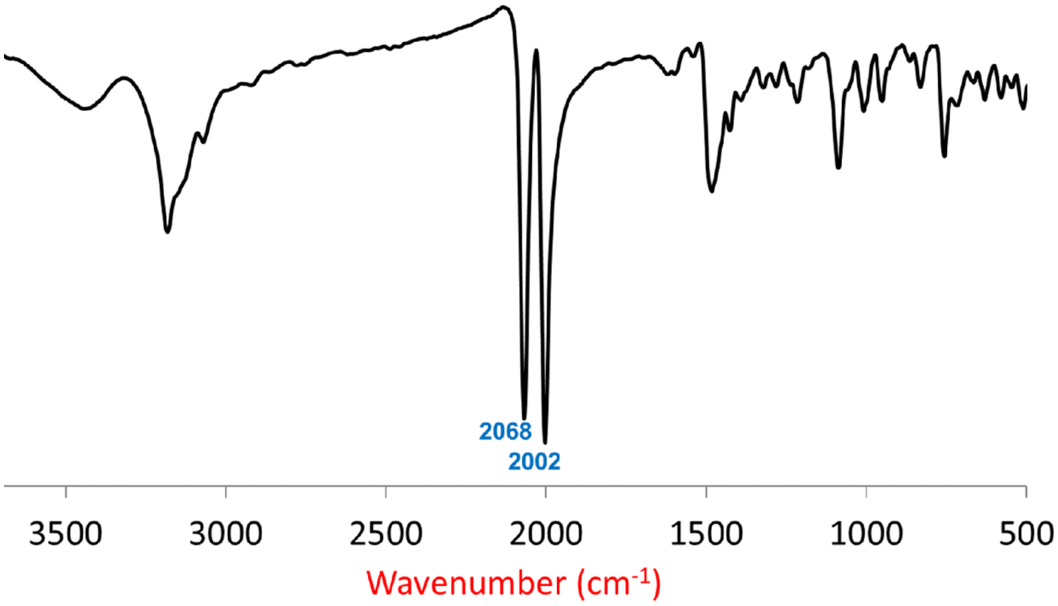
2068
2002
3500
3000
2500
2000
1500
1000
500
Wavenumber (cm-1)

**c)**

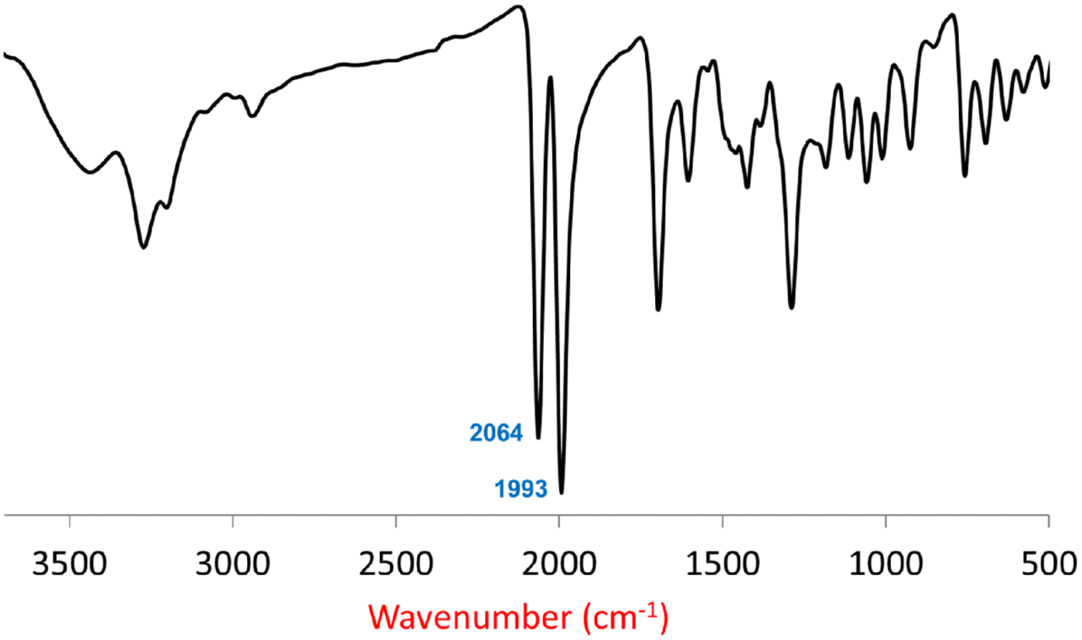
2064
1993
3500
3000
2500
2000
1500
1000
500
Wavenumber (cm-1)

**d)**

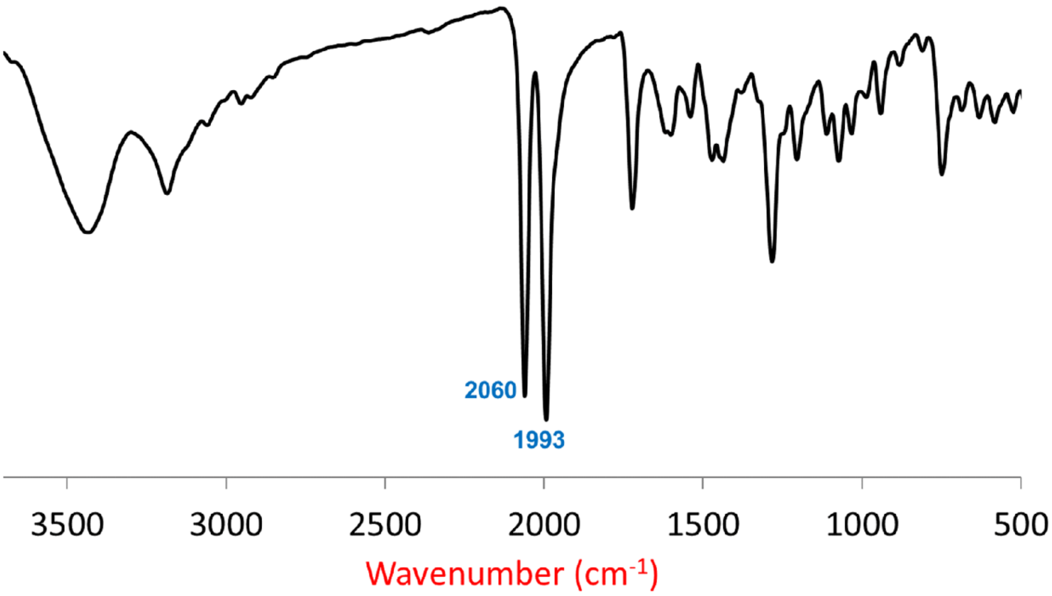

**e)**

**Figure S1** IR spectra of dicarbonyl ruthenium(II) complexes a) **6**, b) **7**, c) **8**, d) **9**, e) **10**.

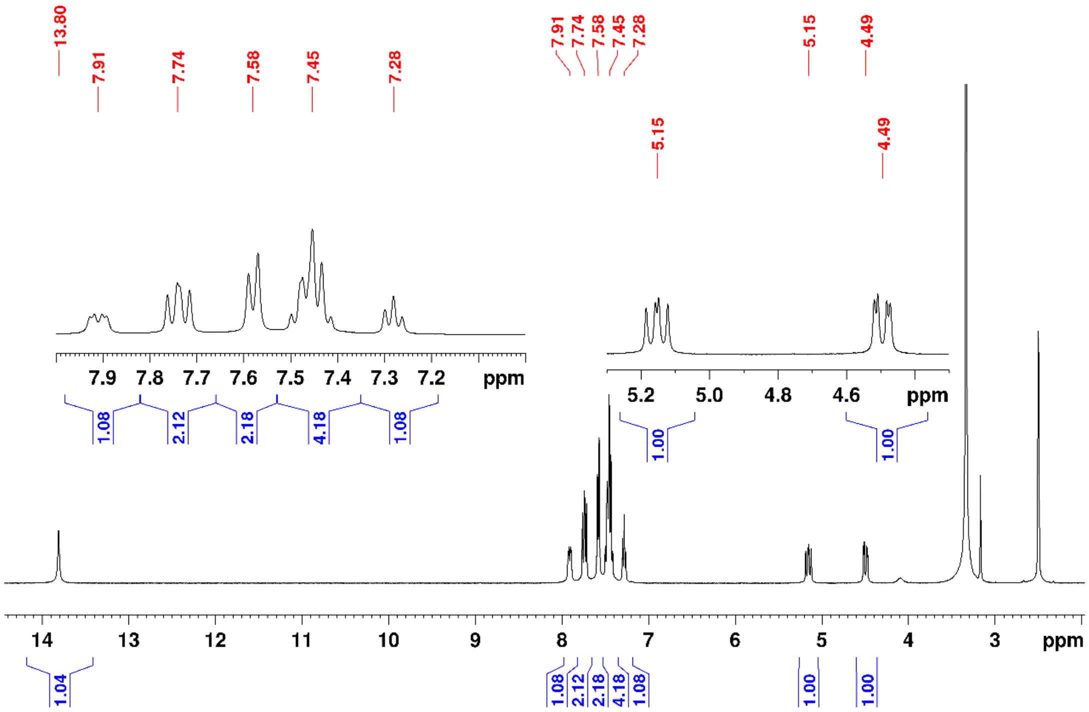
13.80
7.91
7.74
7.58
7.45
7.28
5.15
4.49
1.08
2.12
2.18
4.18
1.08
1.00
1.00
1.04
7.9 7.8 7.7 7.6 7.5 7.4 7.3 7.2 ppm
5.2 5.0 4.8 4.6 ppm
14 13 12 11 10 9 8 7 6 5 4 3 ppm

a)

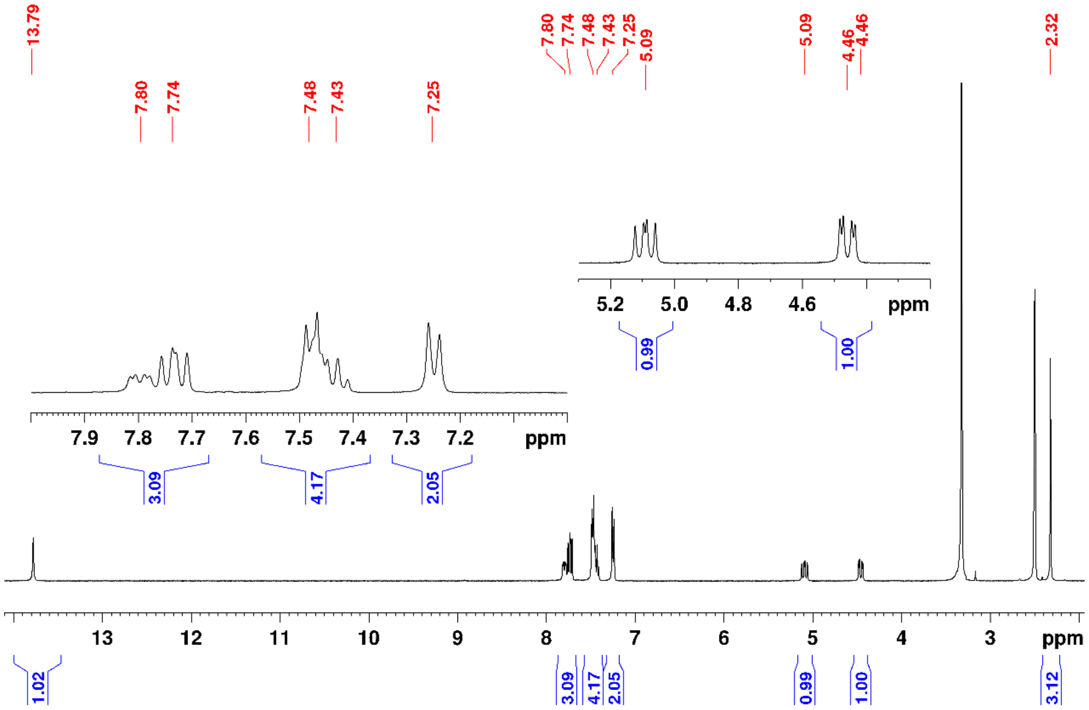
13.79
7.80
7.74
7.48
7.43
7.25
5.09
4.46
4.46
2.32
3.09
4.17
2.05
0.99
1.00
1.02
3.12
7.9 7.8 7.7 7.6 7.5 7.4 7.3 7.2 ppm
5.2 5.0 4.8 4.6 ppm
13 12 11 10 9 8 7 6 5 4 3 ppm

b)

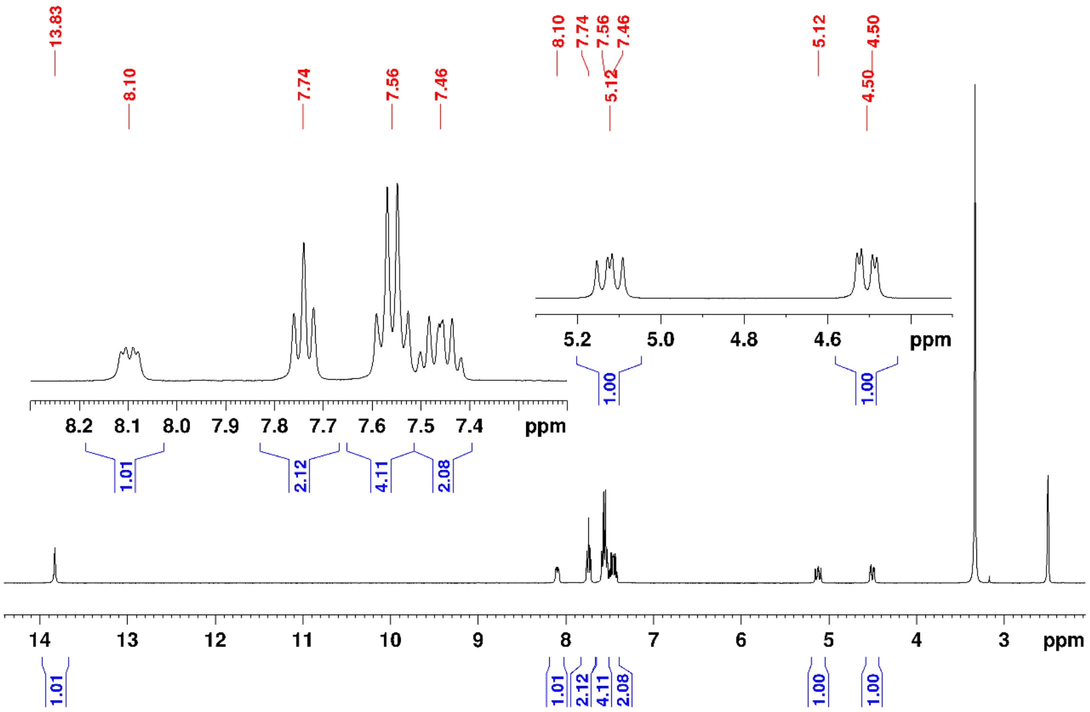
13.83
8.10
7.74
7.56
7.46
5.12
4.50
8.2
8.1
8.0
7.9
7.8
7.7
7.6
7.5
7.4
ppm
1.01
2.12
4.11
2.08
5.2
5.0
4.8
4.6
1.00
14
13
12
11
10
9
8
7
6
5
4
3

c)

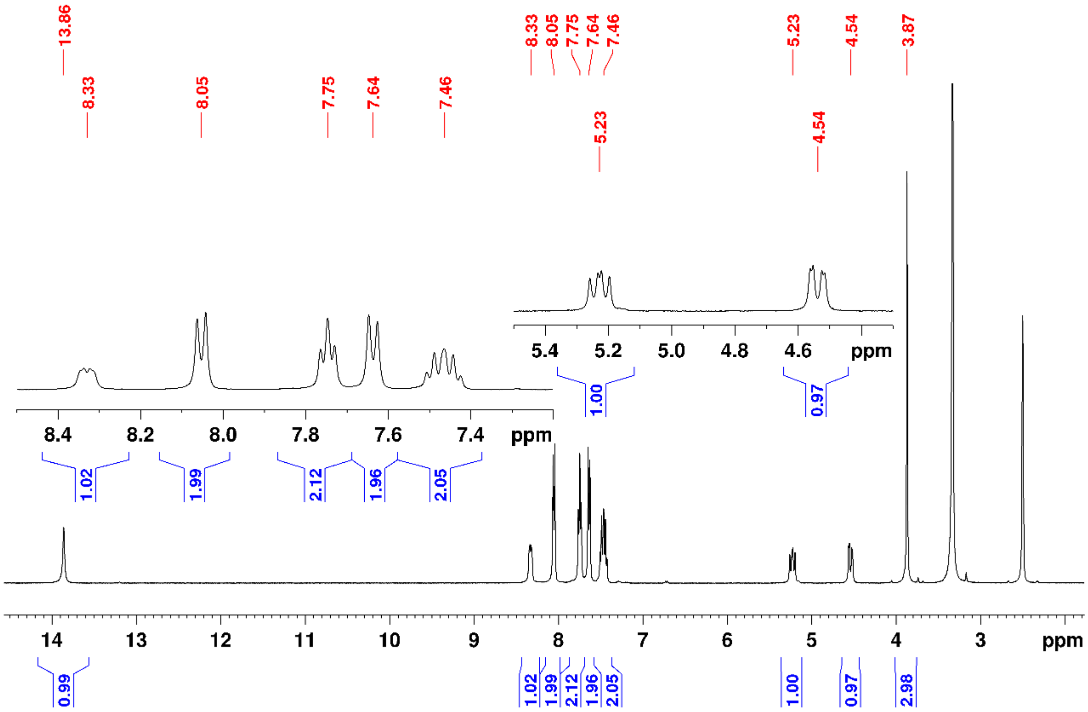
13.86
8.33
8.05
7.75
7.64
7.46
5.23
4.54
3.87
8.4
8.2
8.0
7.8
7.6
7.4
ppm
1.02
1.99
2.12
1.96
2.05
5.4
5.2
5.0
4.8
4.6
1.00
0.97
0.99
2.98
14
13
12
11
10
9
8
7
6
5
4
3

d)

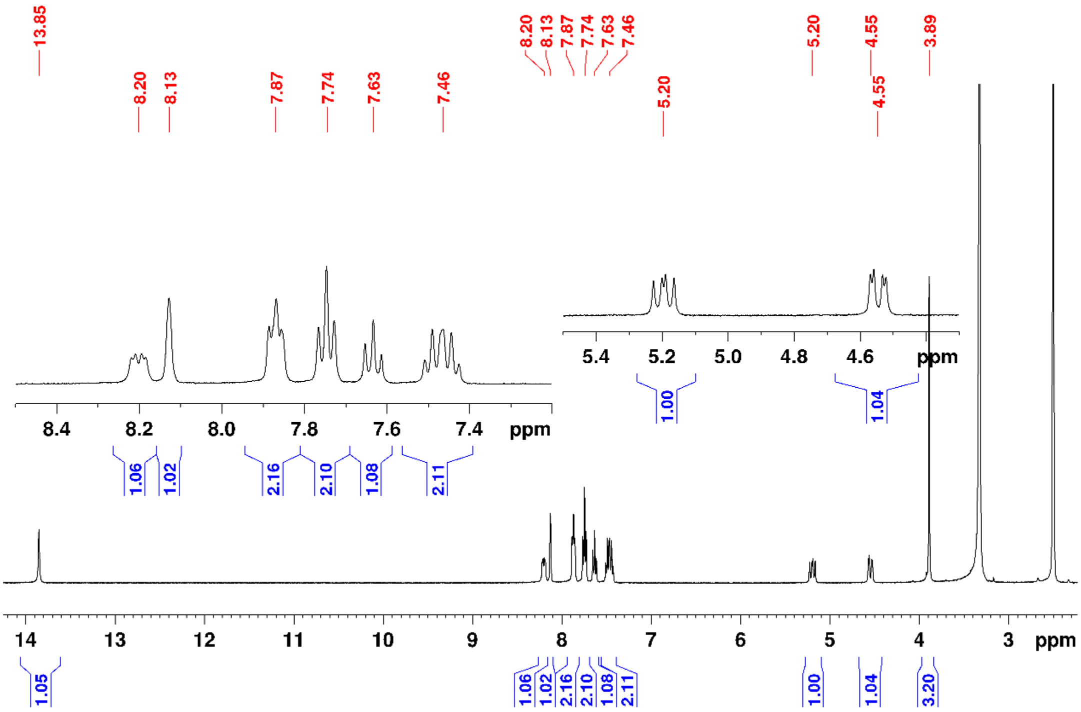

e)

**Figure S2** $^{1}$H NMR spectra of dicarbonyl ruthenium(II) complexes a) **6**, b) **7**, c) **8**, d) **9**, e) **10**.

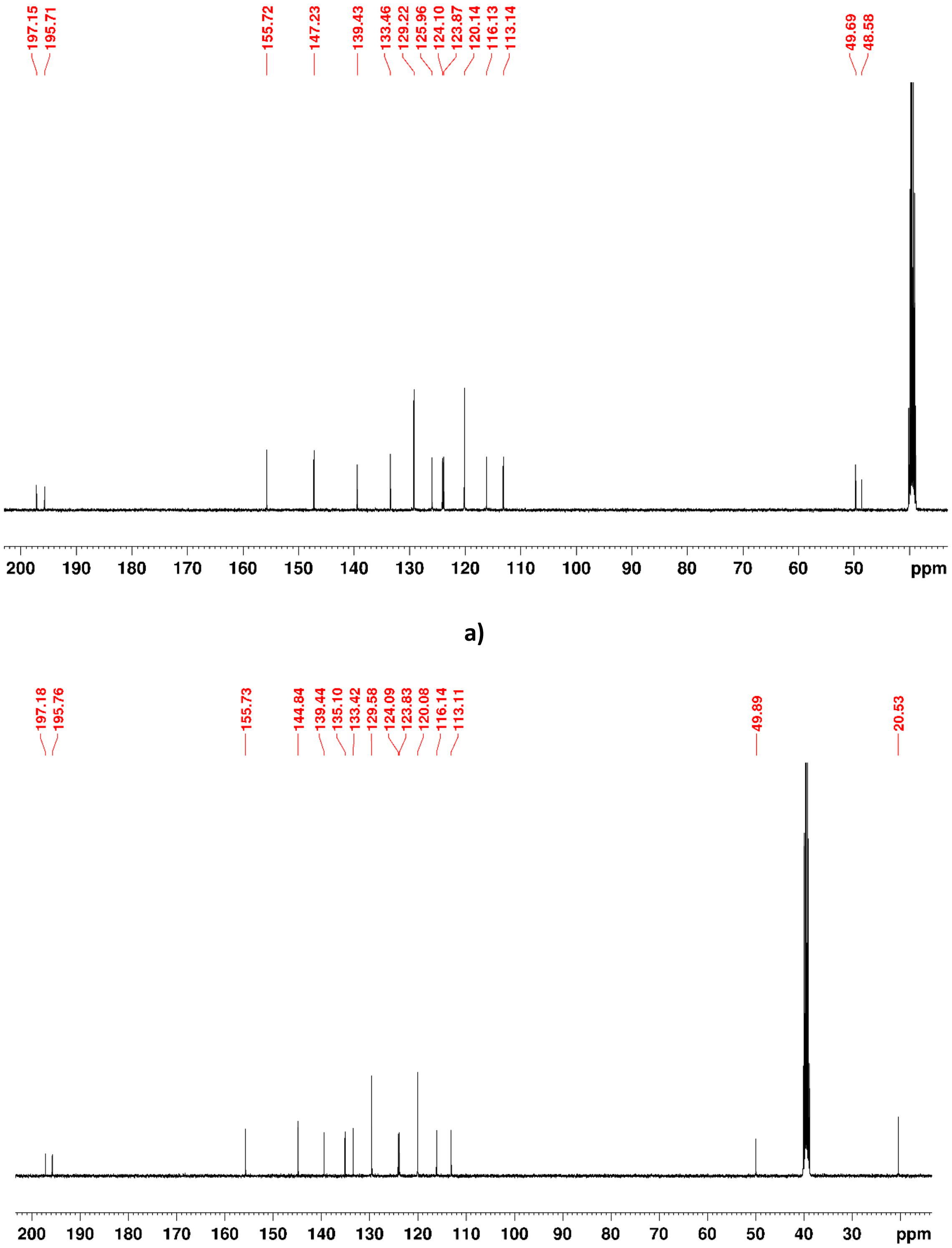

a)

b)

**Figure S3** $^{13}$C NMR spectra of dicarbonyl ruthenium(II) complexes a) **6**, b) **7**.

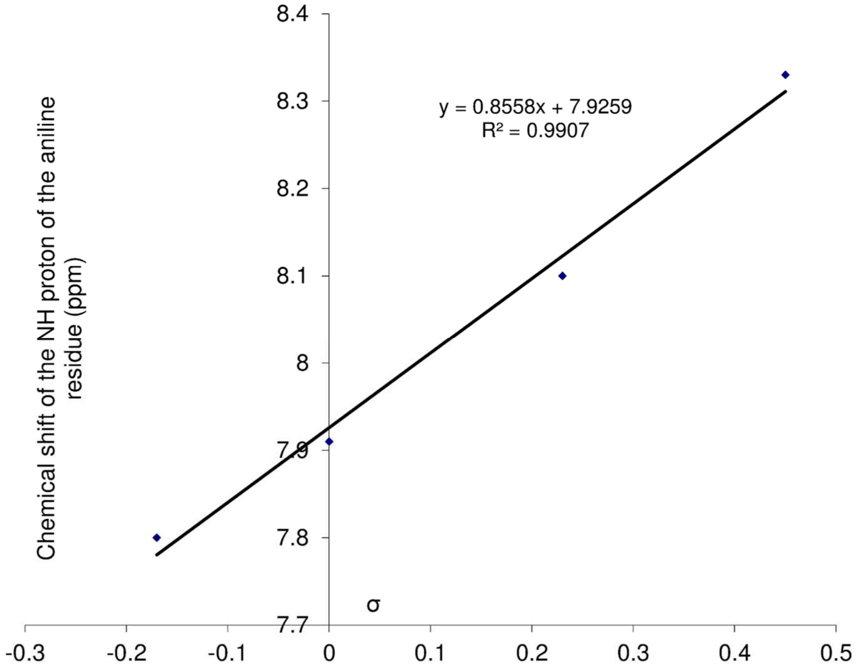

a)

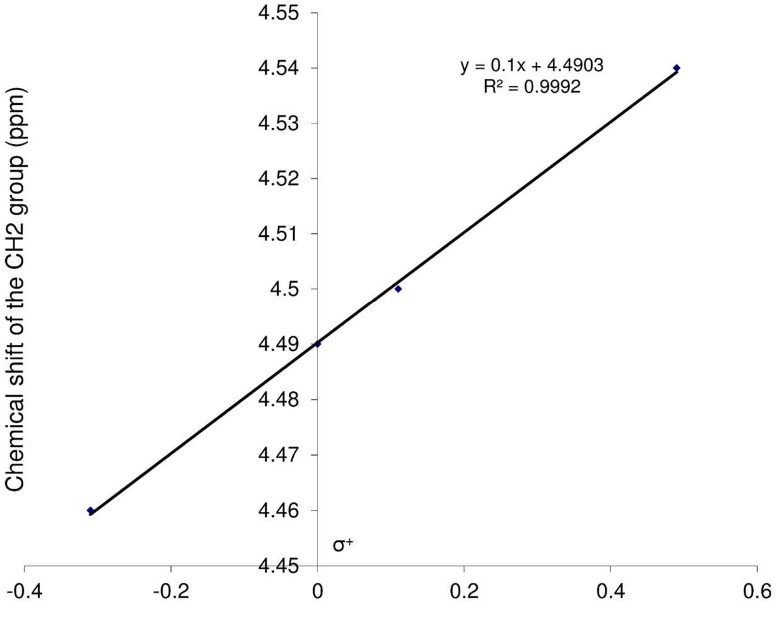

b)

**Figure S4** Hammett plots of the chemical shift of a) NH and b) axial proton of $CH_2$ group as a function of σ and $\sigma^+$, respectively.

**Table S1** Single-crystal X-ray diffraction data and structure refinements of compound **7** and **10**.

| Data | **7** | **10** |
|---|---|---|
| CCDC number | 2085341 | 2085344 |
| Empirical formula | $C_{18}H_{15}Cl_2N_3O_4Ru$ | $C_{17}H_{15}Cl_2N_3O_2Ru$ |
| Formula weight (g·mol$^{-1}$) | 509.30 | 465.29 |
| Temperature (K) | 100.03(17) | 100.01(2) |
| Radiation, λ (Å) | Cu-$K_{\alpha}$, 0.0395 | Cu-K/$_{\alpha}$ 0.71073 |
| Crystal size (mm$^3$) | 0.04 × 0.09 × 0.18 | 0.04×0.11×0.29 |
| Crystal color, habit | Orange block | Clear yellow block |
| Crystal system | Monoclinic | Monoclinic |
| Space group | $P2_1/n$ | $P2_1/n$ |
| $a$ (Å) | 7.86247(9) | 13.75386(13) |
| $b$ (Å) | 11.42684(13) | 8.76188(7) |
| $c$ (Å) | 21.9614(2) | 15.45738(15) |
| $\beta$ (°) | 92.922(2) | 101.9067 |
| Volume (Å$^3$) | 1970.52 | 1822.69 |
| $Z$ | 4 | 4 |
| $\rho_{calc}$ (g·cm$^{-3}$) | 1.717 | 1.696 |
| $F$(000) | 1016 | 928 |
| $\theta$ range (°) | 4.0530 – 77.0920 | 2.9217 – 77.3646 |
| Reflections collected | 16184 | 3806 |
| Parameters / restraints | 254/0 | 227 / 0 |
| [i]GooF on $F^2$ | 1.11870 | 1.07429 |
| [ii]$R_1$ [I>2σ(I)] | 0.0269 | 0.028725 |
| $wR^2$ (all data)[iii] | 0.07138 | 0.082546 |
| Max./min. residual electron density (e·Å$^{-3}$) | 0.448/–0.900 | 0.470 / –1.099 |

[i] Least squares goodness_of_fit

[ii] R_factor_gt. (For each reflection class, the residual factor for significantly intense reflections

[iii] wR_factor_ref. (For each reflection class, the weighed residual factors for all reflections included in the refinement)

**Table S2** Selected experimental bond lengths (Å) and angles (°) of **7** and **10**.

| | **7** | **10** |
|---|---|---|
| Ru–Cl1 | 2.369(6) | 2.403(7) |
| Ru–Cl2 | 2.402(6) | 2.389(6) |
| Ru–N4_1 | 2.102(2) | 2.099(2) |
| Ru–N1_1 | 2.190(2) | 2.192(2) |
| Ru–C1 | 1.868(3) | 1.891(3) |
| Ru–C2 | 1.893(3) | 1.872(3) |
| C1–O1 | 1.131(3) | 1.130(3) |
| C2–O2 | 1.340(4) | 1.133(3) |
| C1–Ru–Cl1 | 91.39(8) | 89.86(8) |
| C1–Ru–Cl2 | 94.49(8) | 93.72(8) |
| C1–Ru–C2 | 87.30(1) | 88.20(1) |
| C1–Ru–N4_1 | 98.93(9) | 99.61(9) |
| C1–Ru–N1_1 | 174.71(9) | 173.86(9) |
| Cl1–Ru–Cl2 | 172.42(2) | 174.48(2) |
| Cl1–Ru–C2 | 91.16(9) | 88.57(7) |
| Cl1–Ru–N4_1 | 86.18(5) | 86.44(5) |
| Cl1–Ru–N1_1 | 89.12(5) | 91.16(5) |
| Cl2–Ru–C2 | 94.05(9) | 95.74(8) |
| Cl2–Ru–N4_1 | 88.03(5) | 89.63(5) |
| Cl2–Ru–N1_1 | 84.56(5) | 84.10(5) |
| C2–Ru–N4_1 | 173.30(1) | 96.64(9) |
| C2–Ru–N1_1 | 98.00(1) | 172.23(9) |
| N4_1–Ru–N1_1 | 75.85(7) | 75.60(6) |

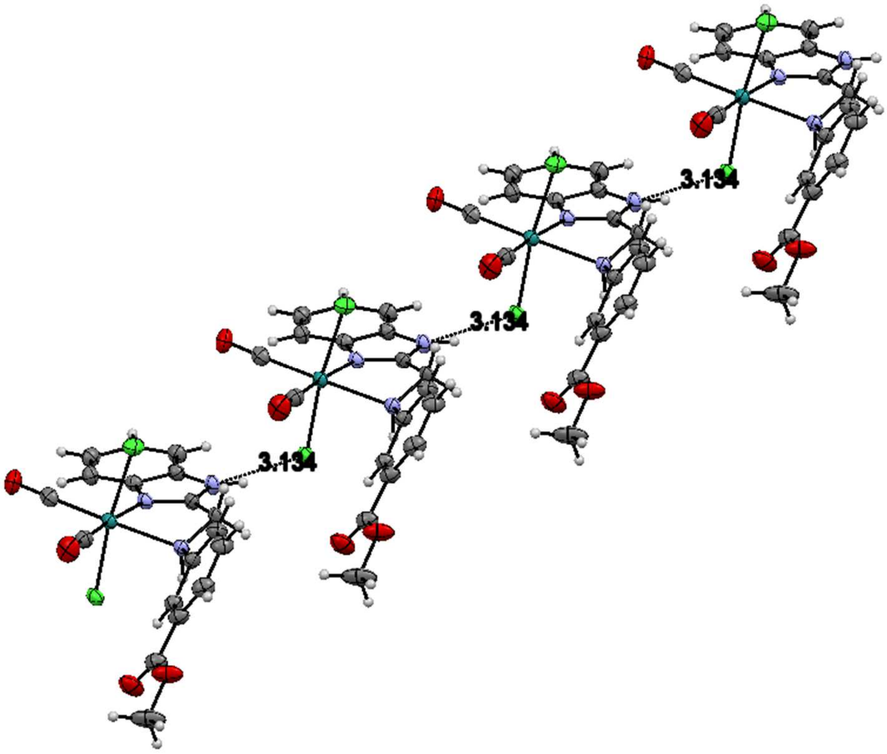

**Figure S5** an infinite chain structure of **10** along the axis ''*c*'' *via* the conventional hydrogen bond interaction.

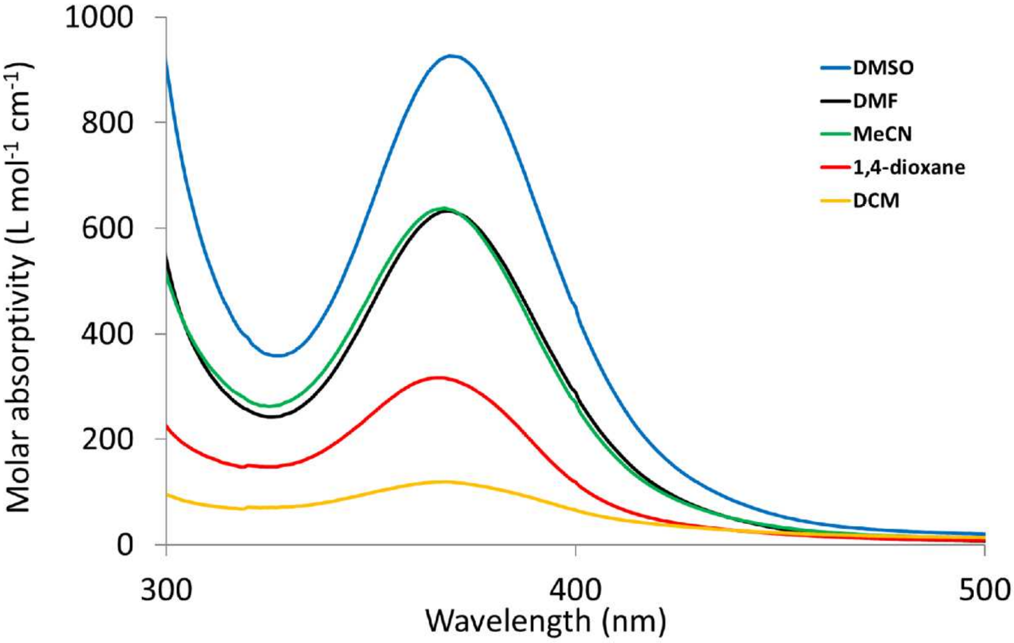

**a)**

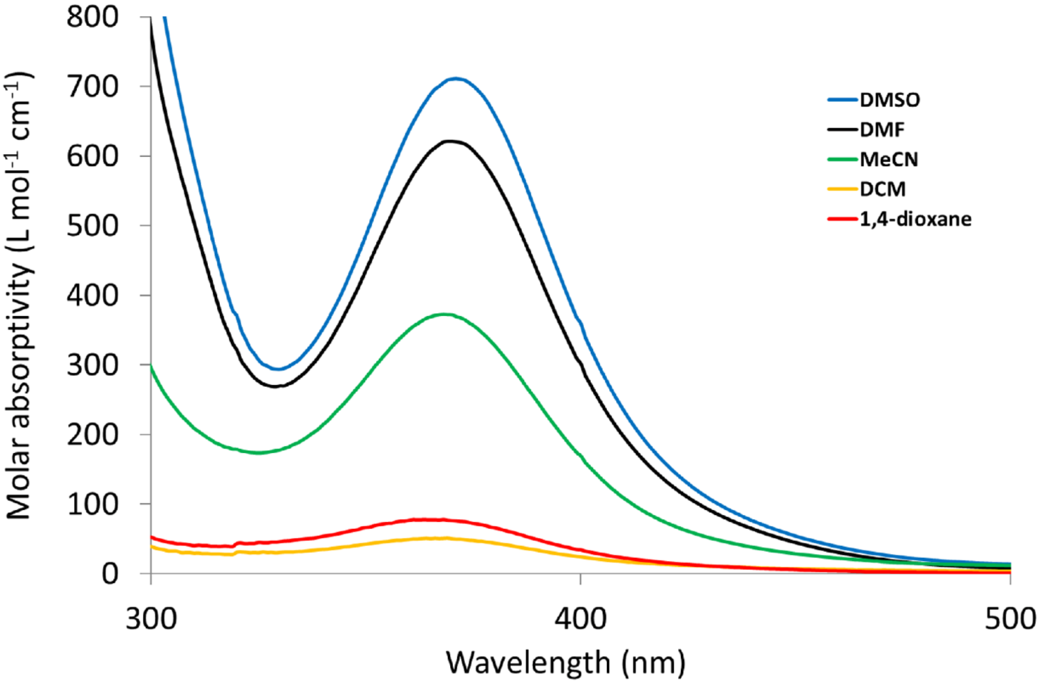

**b)**

**Figure S6** Electronic absorption spectra of a) **7** and b) **9** in different solvents.

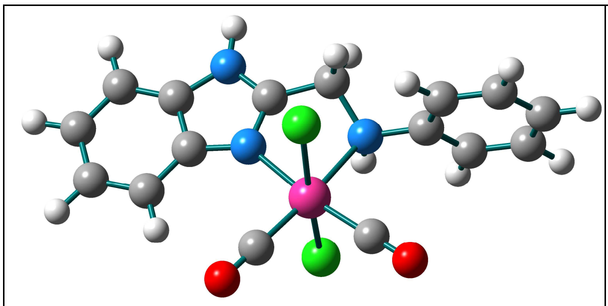

**6**

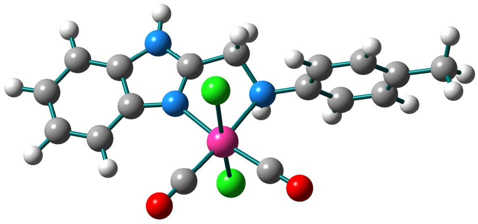

**7**

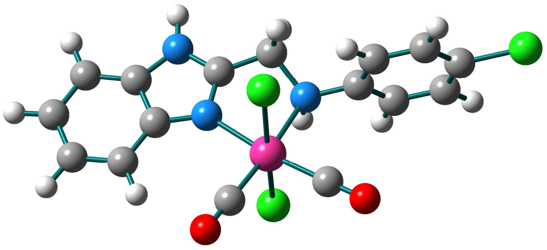

**8**

**9**

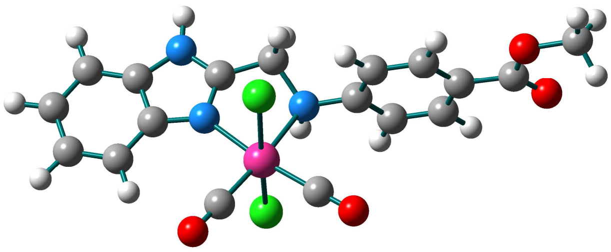

**10**

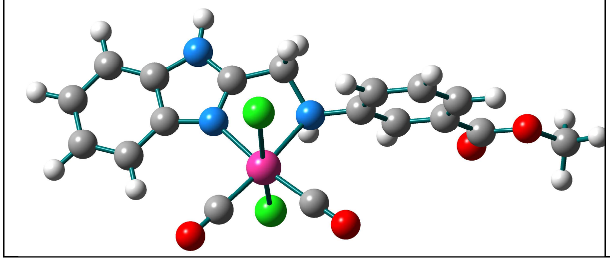

**Figure S7** Local minmum structures of **6–10** obtained at B3LYP/LNAL2DZ level of theory.

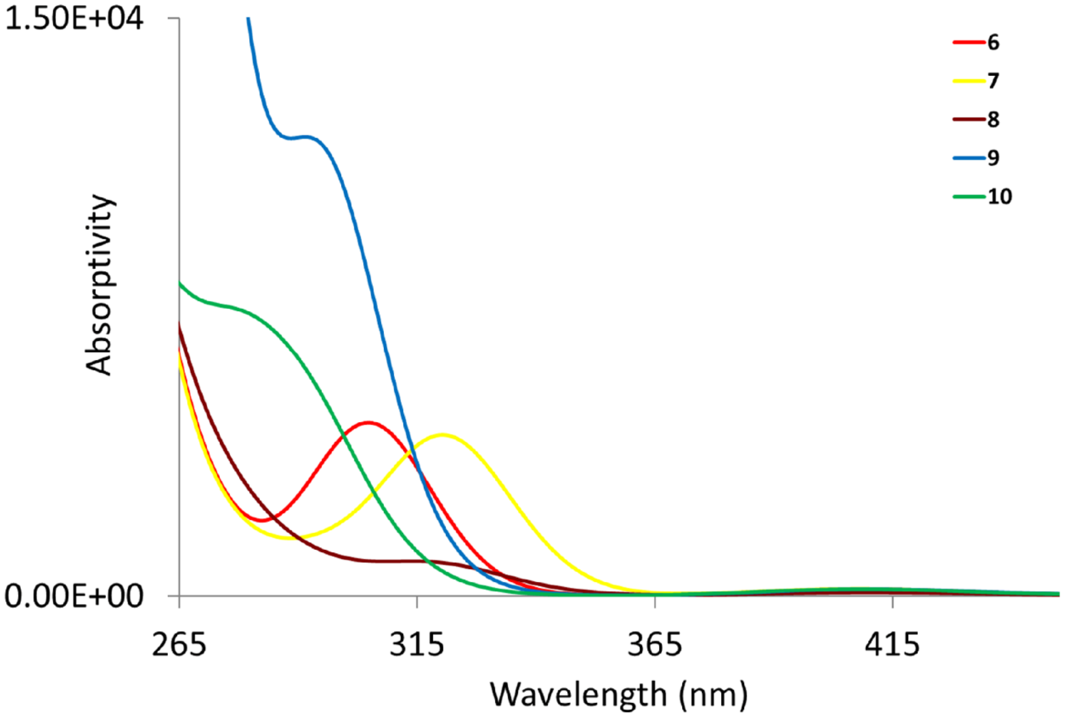

**Figure S8** TD-DFT calculated spectra  of complexes **6**–**10** in the range of 265–415 nm.

**Table S3** Computed excitation energies (eV), electronic transition configurations and oscillator strengths (*f*) of compounds **6**–**10**.

| Energy (cm$^{-1}$) | Wavelength (nm) | *f* | Major contributions |
|---|---|---|---|
| • **6** | | | |
| 23860 | 419 | 0.0007 | HOMO→LUMO (78%) |
| 24749 | 404 | 0.0018 | HOMO–1→LUMO (78%) |
| 31713 | 315 | 0.0002 | HOMO→LUMO+1 (71%) |
| 32152 | 311 | 0.0042 | HOMO–2→LUMO (69%) |
| 32665 | 306 | 0.0484 | HOMO–4→LUMO (23%), HOMO–3→LUMO (57%) |
| 33771 | 296 | 0.0098 | HOMO→L+2 (54%) |
| 38077 | 263 | 0.0148 | HOMO→L+3 (47%) |
| 39668 | 252 | 0.0002 | HOMO→L+5 (29%) |
| 39922 | 250 | 0.0579 | HOMO–4→LUMO+2 (49%), HOMO–3→LUMO+2 (25%) |
| • **7** | | | |
| 23898 | 418 | 0.0007 | HOMO→LUMO (74%) |
| 24766 | 404 | 0.0019 | HOMO–2→LUMO (70%) |
| 31101 | 322 | 0.0528 | HOMO–1→LUMO (81%) |
| 31795 | 315 | 0.0003 | HOMO→LUMO+1 (67%) |
| 32221 | 310 | 0.0042 | HOMO–3→LUMO (68%) |
| 33738 | 296 | 0.0069 | HOMO→LUMO+2 (59%) |
| 35827 | 279 | 0.0006 | HOMO→LUMO+4 (54%) |
| 38023 | 263 | 0.0126 | HOMO→LUMO+3 (62%) |
| 40321 | 248 | 0.0573 | HOMO–4→LUMO+3 (25%), HOMO–2→LUMO+5 (25%) |
| • **8** | | | |
| 236623 | 423 | 0.0002 | HOMO→LUMO (83%) |
| 24528 | 408 | 0.001 | HOMO–1→LUMO (85%) |
| 301436 | 332 | 0.0015 | HOMO→LUMO+2 (69%) |
| 31331 | 319 | 0.0089 | HOMO→LUMO+1 (79%) |
| 31980 | 313 | 0.0004 | HOMO–1→LUMO+1 (25%), HOMO–1→LUMO+2 (60%) |
| 32488 | 308 | 0.0009 | HOMO–1→LUMO+1 (65%), HOMO–1→LUMO+2 (26%) |
| 33297 | 300 | 0.0025 | HOMO→LUMO+3 (39%) |
| 34493 | 289 | 0.0076 | HOMO–5→LUMO (34%), HOMO–2→LUMO (43%) |
| 39643 | 252 | 0.0147 | HOMO–2→LUMO+2 (20%) |
| • **9** | | | |
| 23721 | 422 | 0.0007 | HOMO→LUMO (59%) |
| 24634 | 406 | 0.0018 | HOMO–1→LUMO (61%) |
| 31186 | 321 | 0.0004 | HOMO→L+2 (48%) |

|  |  |  |  |
|---|---|---|---|
| 31692 | 316 | 0.004 | HOMO−2→LUMO (57%) |
| 33120 | 302 | 0.003 | HOMO−3→LUMO (73%) |
| 33207 | 301 | 0.001 | HOMO−1→L+2 (48%) |
| 34098 | 293 | 0.0601 | HOMO−4→LUMO (44%), HOMO→LUMO+3 (29%) |
| 38360 | 261 | 0.387 | HOMO−4→LUMO+1 (72%) |
| • **10** |  |  |  |
| 23887 | 419 | 0.0007 | HOMO→LUMO (58%) |
| 24754 | 404 | 0.0018 | HOMO−1→LUMO (62%) |
| 31299 | 319 | 0.0003 | HOMO→LUMO+2 (42%) |
| 32033 | 312 | 0.0035 | HOMO−2→LUMO (57%) |
| 33059 | 302 | 0.0002 | HOMO−1→LUMO+1 (37%), HOMO−1→LUMO+2 (28%) |
| 33139 | 302 | 0.0028 | HOMO→LUMO+1 (43%), HOMO→LUMO+2 (27%) |
| 33812 | 296 | 0.0223 | HOMO→LUMO+3 (43%) |
| 35918 | 278 | 0.0021 | HOMO→LUMO+5 (60%) |
| 38174 | 262 | 0.009 | HOMO→LUMO+4 (56%) |
| 39198 | 255 | 0.0067 | HOMO−3→LUMO+2 (34%), HOMO−1→LUMO+4 (24%) |

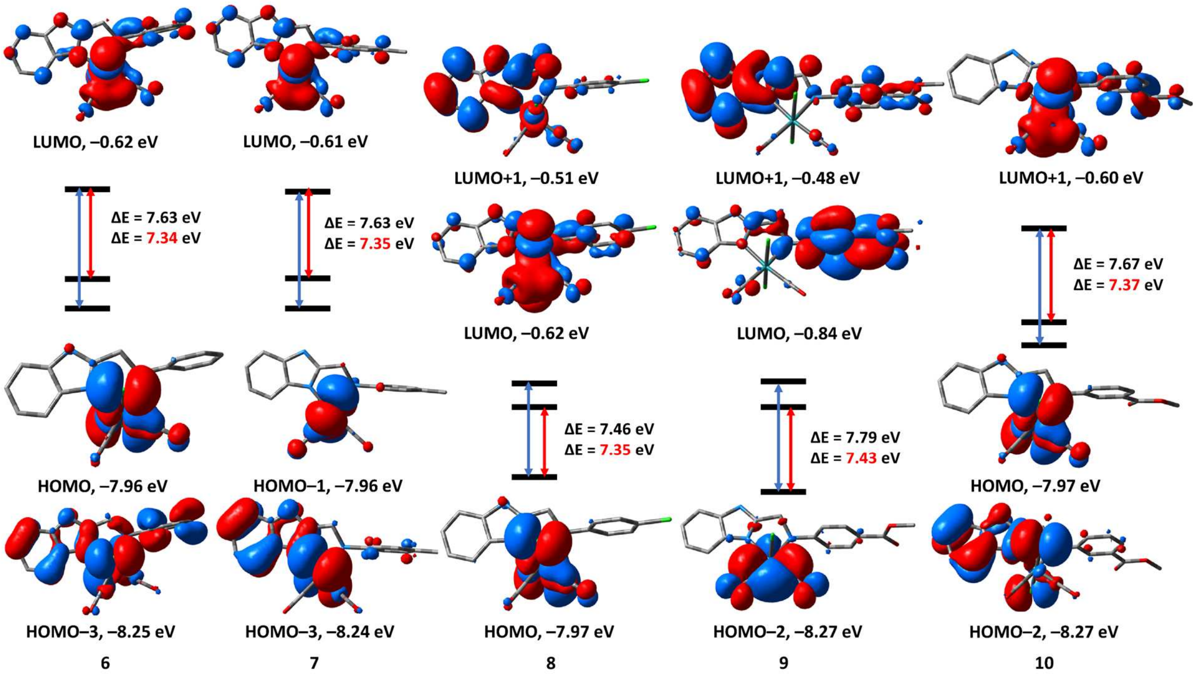

**Figure S9** Selected FMO's orbitals of **6–10** calculated at CAM-B3LYP/LANL2DZ level of theory.

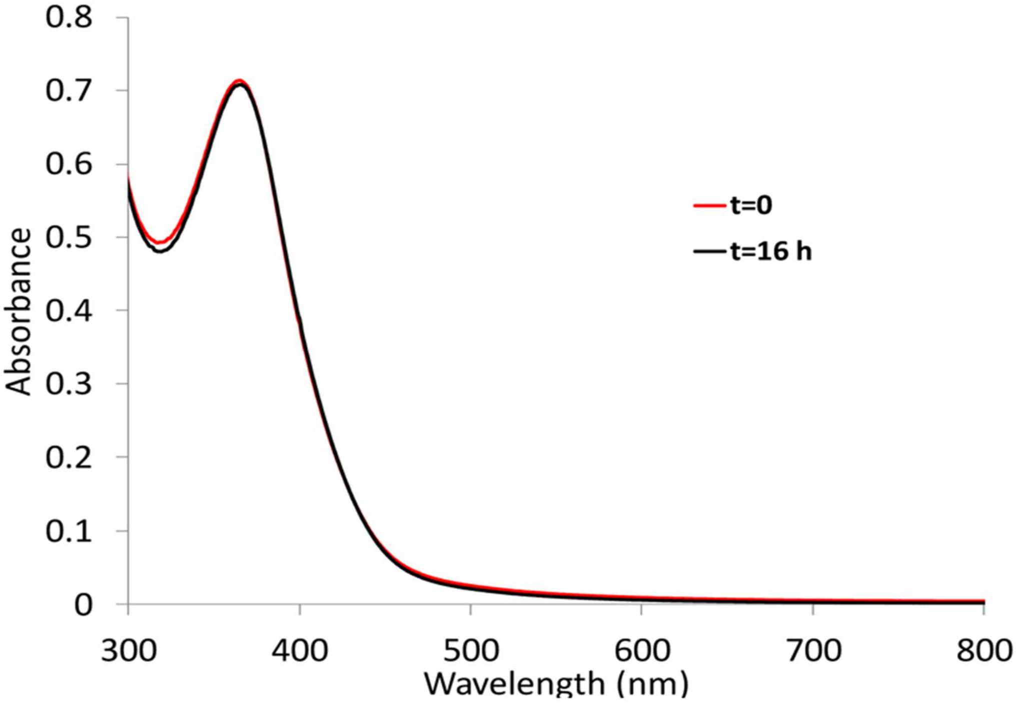
0.8
0.7
0.6
0.5
0.4
0.3
0.2
0.1
0
Absorbance
300
400
500
600
700
800
Wavelength (nm)
t=0
t=16 h

**a)**

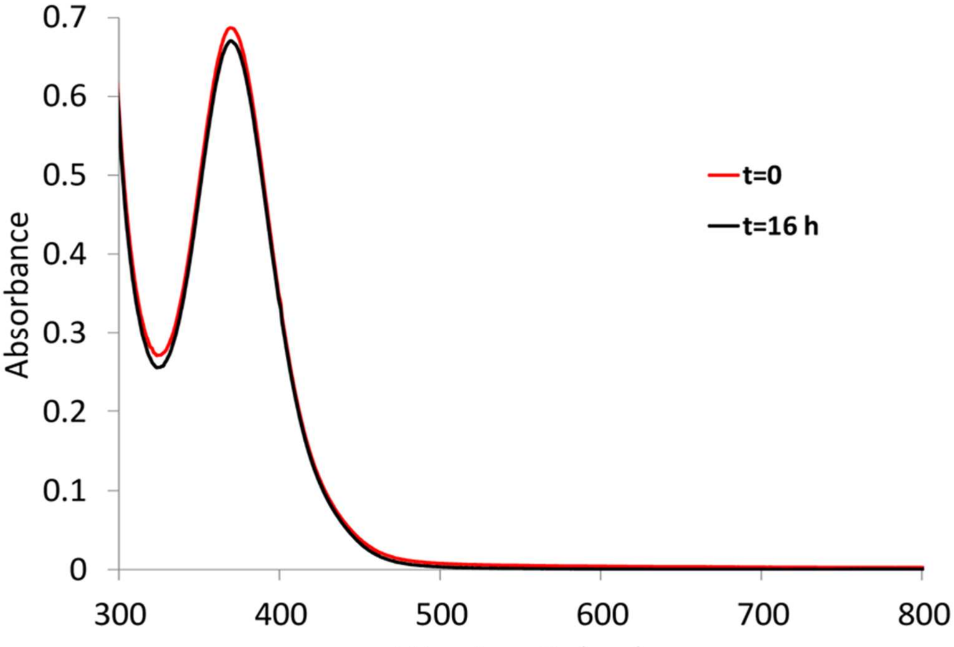
0.7
0.6
0.5
0.4
0.3
0.2
0.1
0
Absorbance
300
400
500
600
700
800
Wavelength (nm)
t=0
t=16 h

**b)**

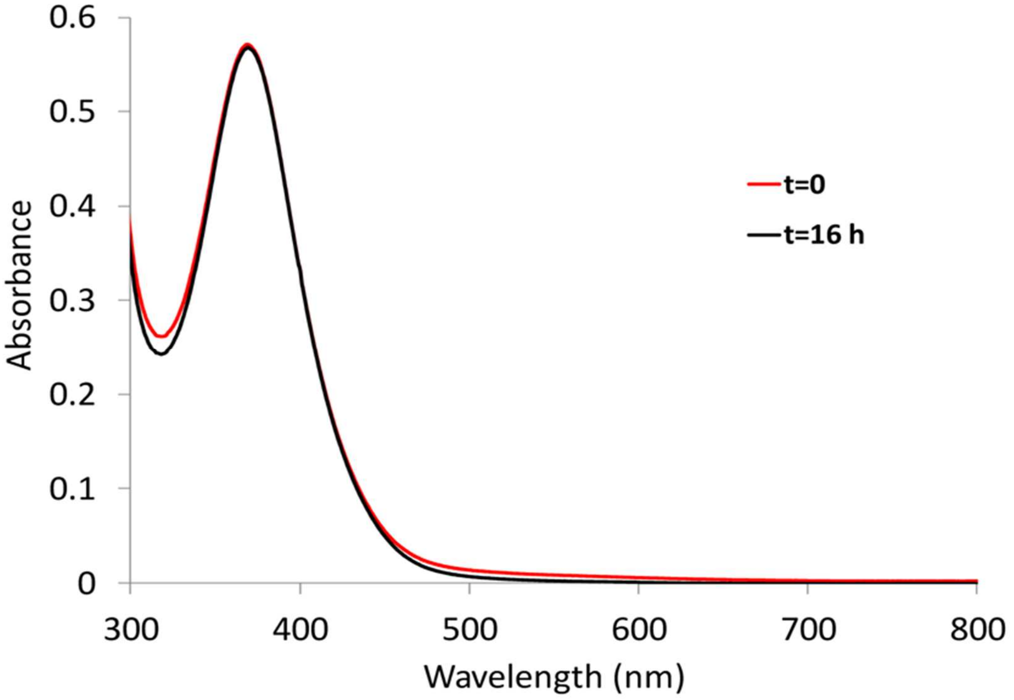
0.6
0.5
0.4
0.3
0.2
0.1
0
Absorbance
t=0
t=16 h
300
400
500
600
700
800
Wavelength (nm)

c)

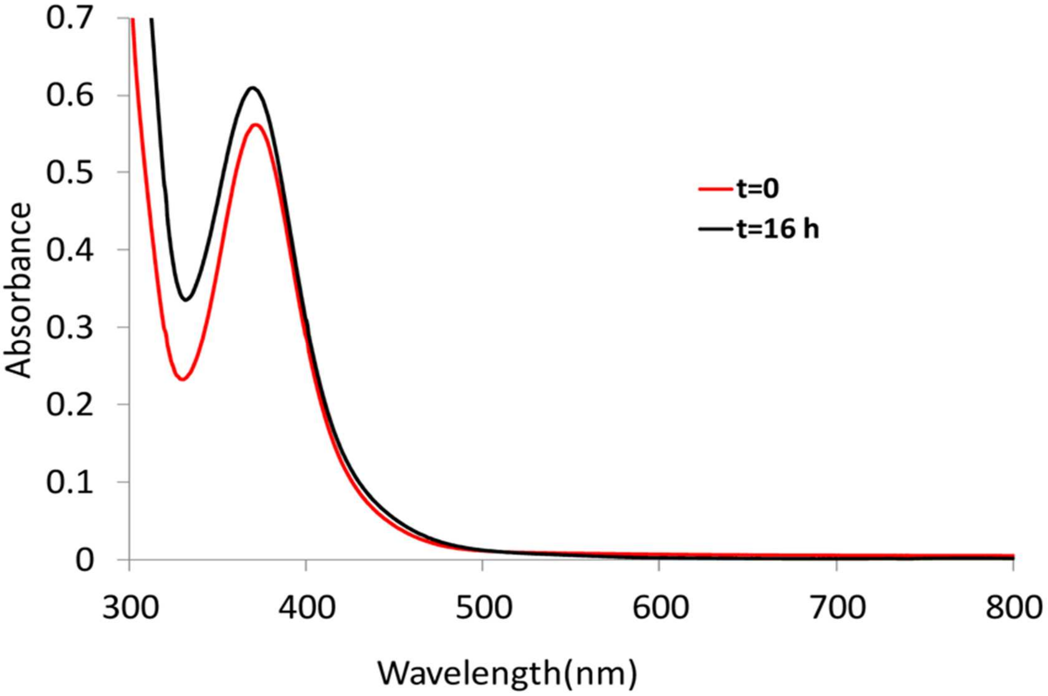
0.7
0.6
0.5
0.4
0.3
0.2
0.1
0
Absorbance
t=0
t=16 h
300
400
500
600
700
800
Wavelength(nm)

d)

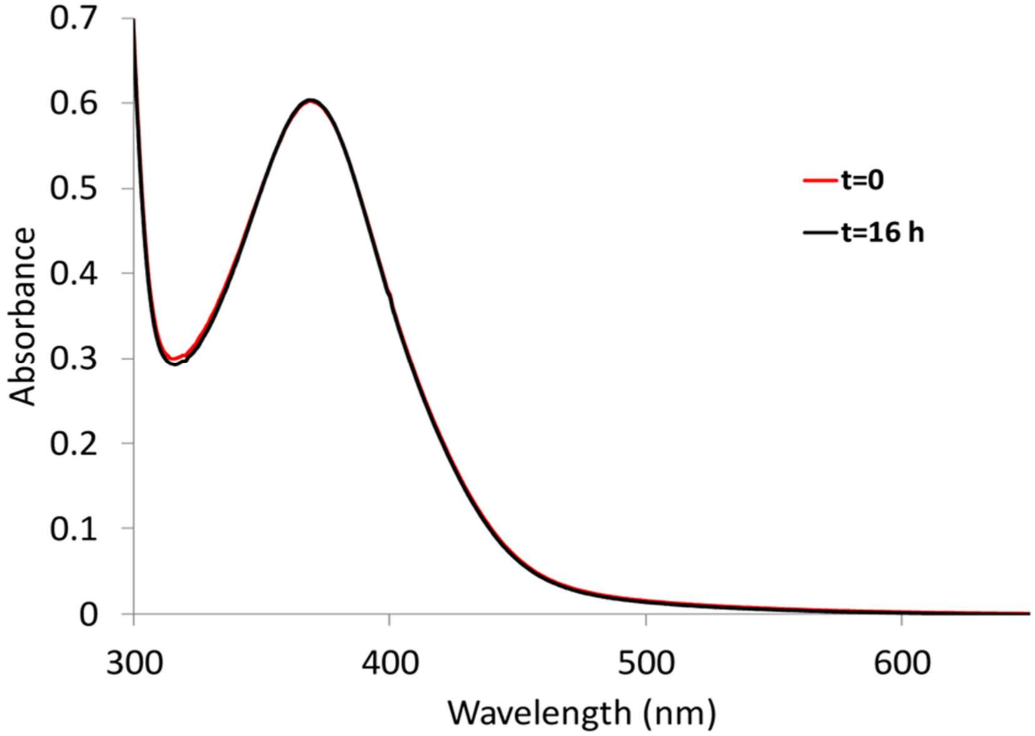

**e)**

**Figure S10** Electronic absorption changes upon incubation of complexes a) **6** (0.4 mM), b) **7** (0.86 mM), c) **8** (0.70 mM), d) **9** (0.84 mM), and e) **10** (1.2 mM) in DMSO in the dark for 16 h.

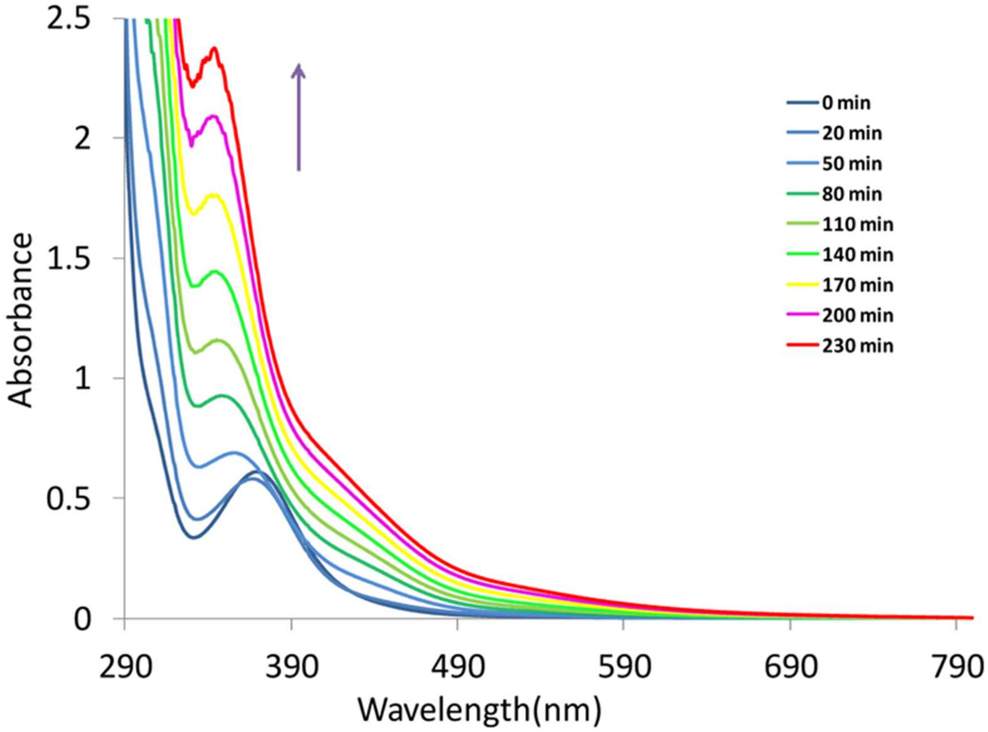

**Figure S11** UV/Vis spectral changes of **9** (0.84 mM in DMSO) upon photolysis at 365 nm with increasing illumination time (0–230 min).

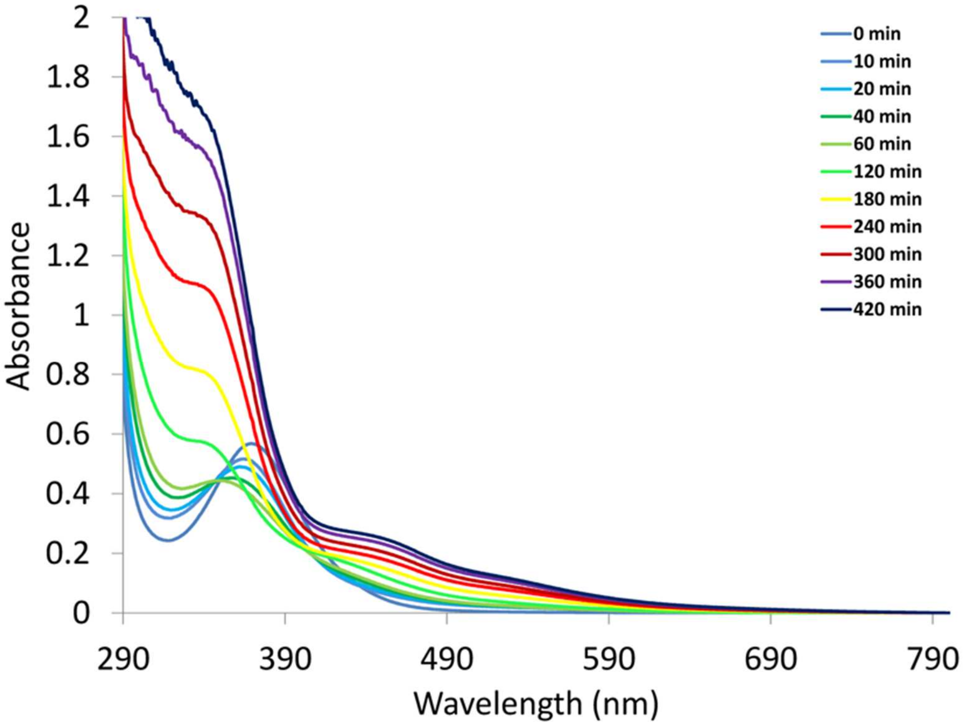

**a)**

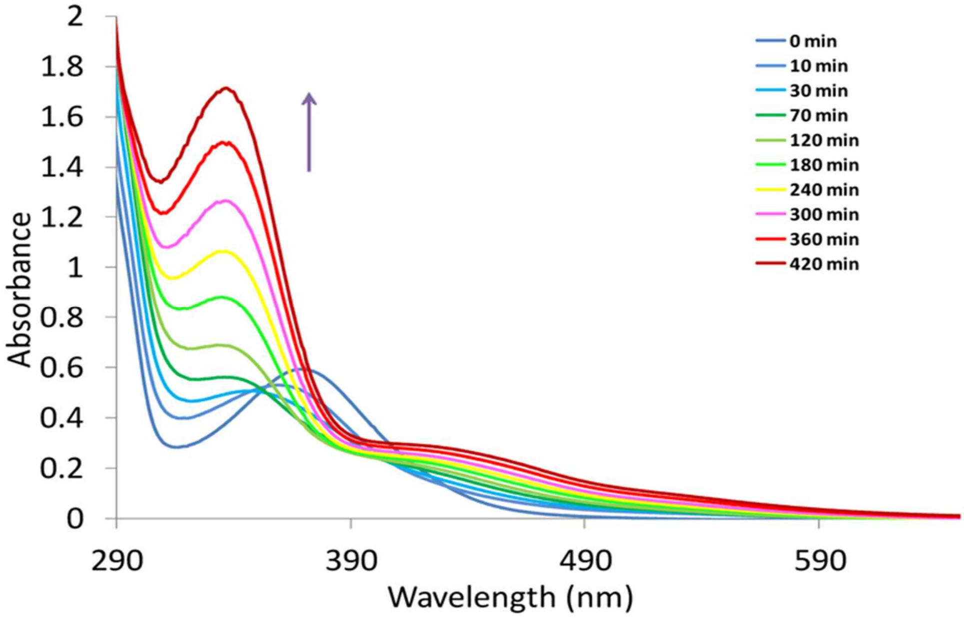

**b)**

**Figure S12** UV/Vis spectral changes of a) **8** (0.70 mM in DMSO) and b) **10** (0.86 mM in DMSO) upon photolysis at 365 nm with increasing illumination time (0–420 min).

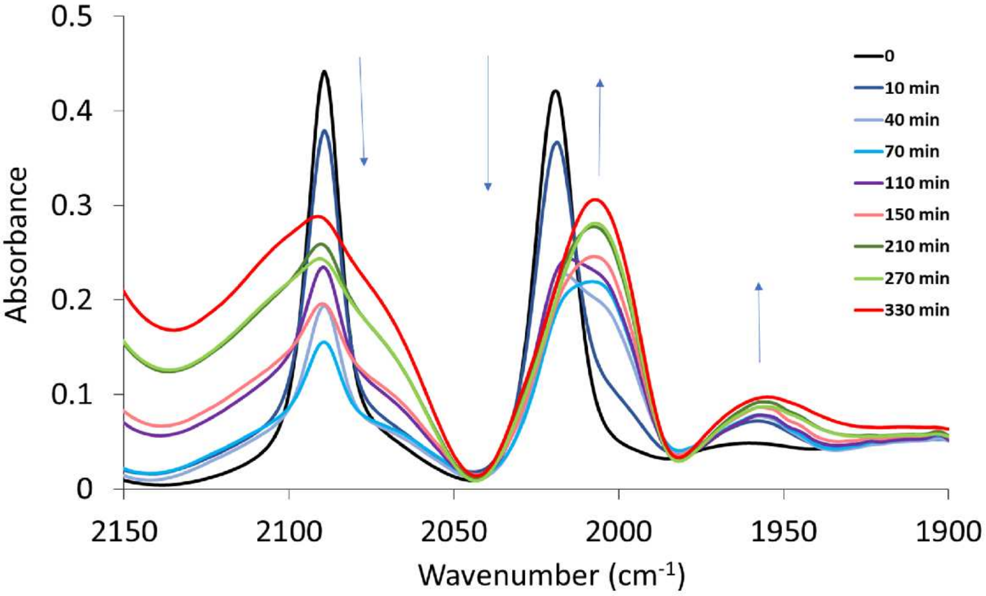
0.5
0.4
0.3
0.2
0.1
0
Absorbance
2150
2100
2050
2000
1950
1900
Wavenumber (cm$^{-1}$)
0
10 min
40 min
70 min
110 min
150 min
210 min
270 min
330 min

a)

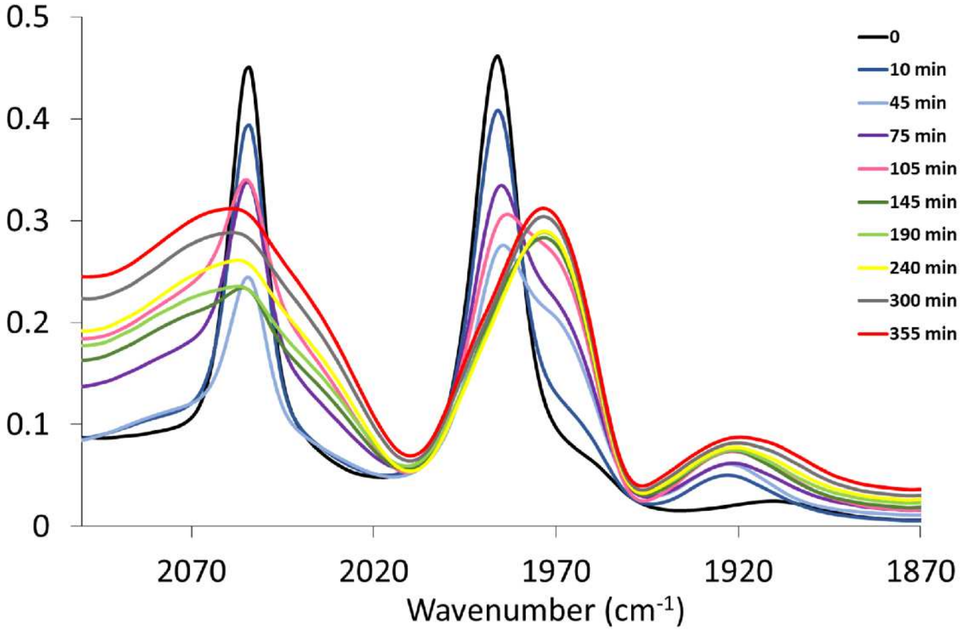
0.5
0.4
0.3
0.2
0.1
0
2070
2020
1970
1920
1870
Wavenumber (cm$^{-1}$)
0
10 min
45 min
75 min
105 min
145 min
190 min
240 min
300 min
355 min

b)

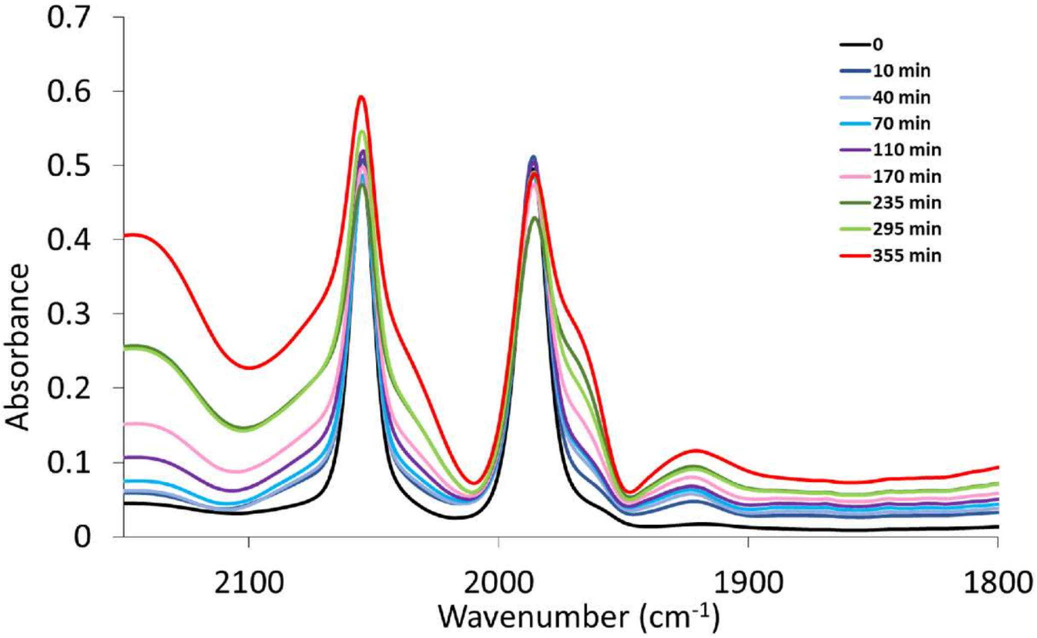

**c)**

**Figure S13** Time-dependent changes in the FTIR spectra of a) **7**, b) **8**, and d) **10** (8 mM in DMSO) upon exposure to light source at 365 nm with increasing illumination time (0–330, 0–355, and 0–355 min, respectively).

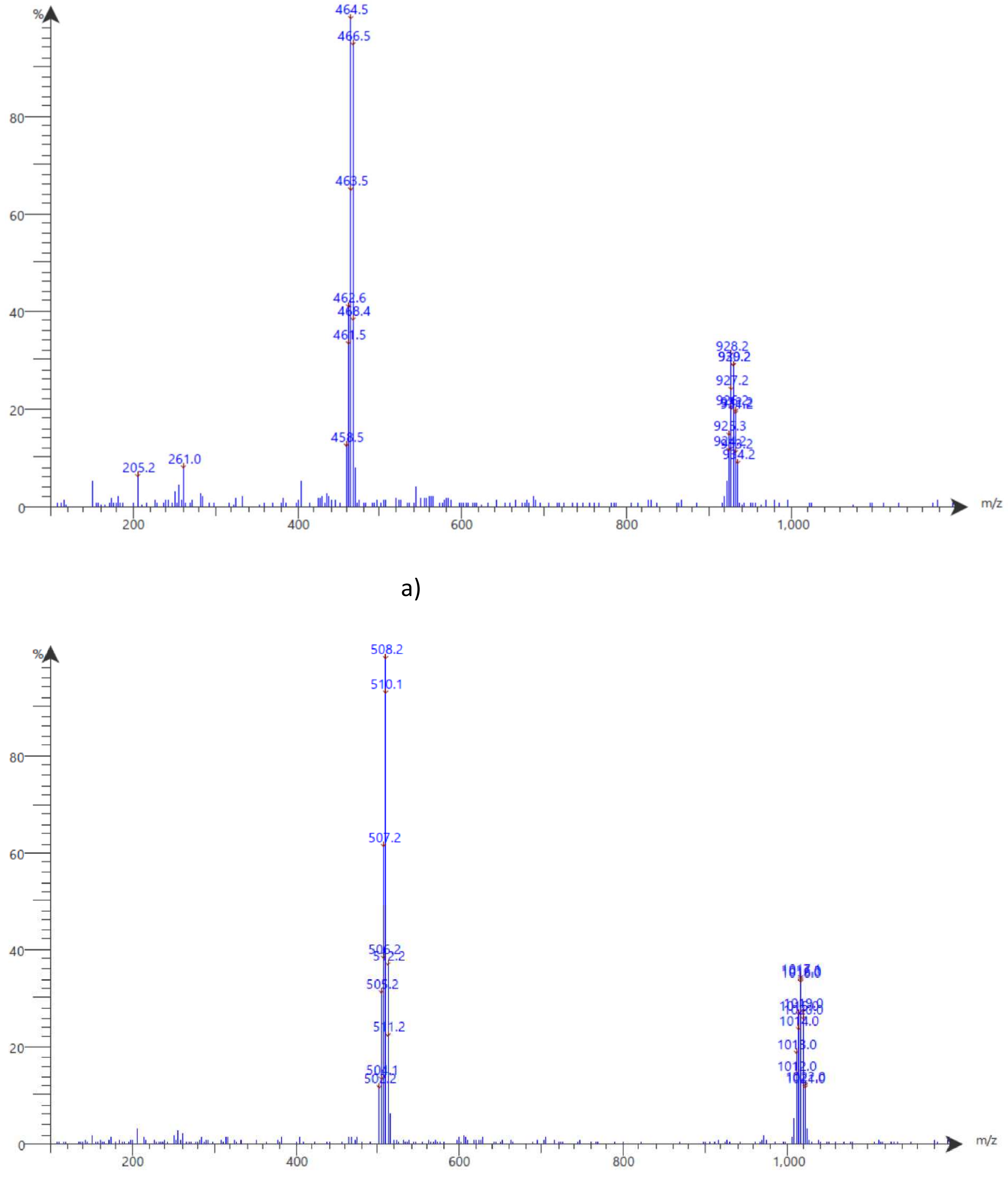

**Figure S14** Negative mode ESI MS spectra of a) **7** and b) **10**.